From midplane to planets : the chemical fingerprint of a disk
Eistrup, C.

Citation
Eistrup, C. (2018, October 16). *From midplane to planets : the chemical fingerprint of a disk*.
Retrieved from https://hdl.handle.net/1887/66260

Version:	Not Applicable (or Unknown)
License:	[Licence agreement concerning inclusion of doctoral thesis in the Institutional Repository of the University of Leiden](https://hdl.handle.net/1887/66260)
Downloaded from:	https://hdl.handle.net/1887/66260

Note: To cite this publication please use the final published version (if applicable).

Cover Page

Universiteit Leiden

Author: Eistrup, C.
Title: From midplane to planets : the chemical fingerprint of a disk
Issue Date: 2018-10-16

5 Matching protoplanetary disk midplane chemical evolution to cometary compositions

A chemical evolution taxonomy for comets

C. Eistrup, C. Walsh, D. Carr, M. Drozdovskaya & E.F. van Dishoeck

Abstract - Comets are planetesimals left over from the formation

of planets in the Solar System. They reside far away from the Sun, and are built up of pristine ices that may trace the chemical history of the Solar System. With a growing number of observed molecular abundances in many comets, and an improved understanding of chemical evolution in protoplanetary disk midplanes, comparisons can be made between models and observations, that could potentially constrain the formation histories of comets.

Aim: To carry out the first statistical comparison between cometary volatile ice abundances and modelled evolving abundances in a protoplanetary disk midplane. A χ^2-method is used to determine maximum likelihood surfaces for 15 different comets to have formed at a given time (up to 8 Myr) and place (out to 30 AU) in the pre-Solar nebula midplane.

Methods: This is done using observed volatile abundances for 15 comets, and the evolution of volatile abundances from chemical modelling in disk midplanes. Two assumptions for the chemical modelling starting conditions (cloud inheritance or chemical reset), as well as two different sets of cometary species (parent species, with or without sulphur species) are investigated.

Results: When considering all parent species (ten molecules) in the reset scenario the χ^2 likelihood surfaces show a characteristic trail in the parameter space with high likelihood of formation between 30 AU at early times and 15 AU at later times, for five comets. This trail roughly traces the CO iceline. For the inheritance scenario, somewhat good agreement is found for five comets, suggesting they formed inside 15 AU. When only considering carbon and oxygen bearing species good agreement is found for ten comets for the reset scenario, also suggesting they formed at or inside the CO iceline, but possibly at different times during the 8 Myr timescale. Comparing the carbon and oxygen bearing species to the inheritance scenario also shows the same trends as for the inheritance scenario with the full sample of species considered.

Conclusions: A statistical comparison between observed and modelled chemical abundances in comets and comet-forming regions is potentially a powerful tool for constraining cometary formation histories. Reducing the number of considered species to only carbon and oxygen bearing species (seven species in total) constrains the formation of 14 out of 15 comets to the vicinity of the CO iceline (moving from ∼30 to ∼15 AU over time), with chemistry having been (partially) reset early in the pre-Solar nebula. These comets did not previously fall into the same taxonomical categories together, therefore this chemical constraint may be proposed as an alternative taxonomy for comets. Based on the most likely time for each of these comets to have formed during the disk chemical evolution, a formation time classification for these 14 comets is proposed.

5.1   Introduction

When the Solar System formed 4.6 billion years ago, the planets formed their cores from solid material in the pre-Solar nebula. In the outer, colder regions of this nebula volatile molecules such as H_2O, CO_2 and CO were frozen out as ices on the surfaces of grains, and later larger bodies. Some of these bodies merged to form the planetary cores, and eventually the Jovian planets, but some of this solid material remained unused by planets, and is still present in our Solar System today as comets.

Comets are made up of partly refractory dust and partly volatile ices. These ices reside deep inside the comets, and they are thought to be pristine samples of the material that was present in the pre-Solar nebula (see review by Mumma & Charnley 2011). Comets are thus interesting because of what they can tell us about the chemical composition in the icy outer pre-Solar nebula 4.6 billion years ago, but also because comets are known to have impacted on the Earth, after having been dynamically scattered towards the Sun from the outer Solar System. The material (volatile and organic) they carry on them has thus added to the chemical make-up of the Earth, and understanding the origin of water and life on the Earth may have traces back to comets.

Comets have been observed from the ground and from space for decades, in various wavelength regimes. Several efforts have gone into detecting molecular species in the comae of comets, and using these to classify them (A'Hearn et al. 1995; Fink 2009; Mumma & Charnley 2011; Cochran et al. 2012; Le Roy et al. 2015). At least two classification groups have been proposed for cometary compositions: "Typical" and "Depleted", where "Depleted" refers to a depletion in organic carbon-chain molecules, compared with the "Typical" compositions (see e.g. Cochran et al. 2012). Hundreds of comets have been analysed for composition. The majority of these (75-91%) fall under the "Typical" category, as found by Cochran et al. (2012). They also find good agreement with the other studies (e.g. A'Hearn et al. 1995; Fink 2009) as to which comets are depleted, and which are not.

However, relating observed cometary species to the actual cometary compositions remains a challenge. This is because some parent species (e.g. NH_3 and HCN) sublimating from the comet get dissociated into chemical daughter species, such as radicals (e.g. NH_2 and CN for parent species NH_3 and HCN, respectively), when moving from the surface to the coma of the comet. Tracing which daughter species originate from which parent species, and how the daughter species abundance in the coma translates to parent species' abundances near the surface is tricky, as pointed out by e.g. Le Roy et al. (2015).

Recently, ESA's *Rosetta* mission visited comet 67P, and orbited the comet for two years with an armada of instruments, providing unprecedented details about the comet. The ROSINA instrument has been particularly powerful for determing chemical composition. The comet showed very different amounts of produced species from the summer to the winter hemispheres (Le Roy et al. 2015), and hence it is difficult to say which amounts of which species are representative of the bulk composition, since temperature plays a role. It is in turn difficult to classify
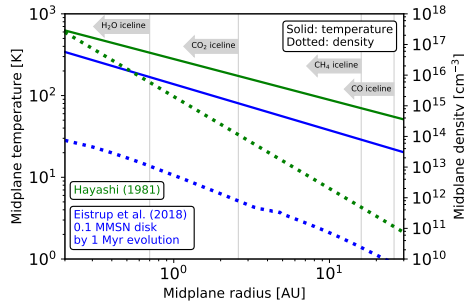
Figure 5.1: Physical structures of the disk midplanes for the pre-Solar nebula from Hayashi (1981) (in green), and for the 0.1 MMSN disk by 1 Myr evolution from Eistrup et al. (2018) (in blue). Solid profiles are for temperature. Dotted profiles are for number density. The vertical grey lines indicate the positions of the icelines of H_2O, CO_2, CH_4 and CO by 1 Myr evolution for the 0.1 MMSN disk in Eistrup et al. (2018). The grey arrows on each of the vertical lines indicate which species each line is associated with, and how the iceline moves over time (all inwards).

this comet's composition according to the "Typical"-and-"Depleted"-scheme.

In this work, a quantitative comparison between the observed cometary abundances and the protoplanetary disk midplane chemical evolution models from Eistrup et al. (2018) will be made. Molecular abundances, observed mainly from remote sensing with infrared (IR) and mm telescopes, for each of the 15 comets presented in Le Roy et al. (2015) will be compared statistically in time and space with volatile abundances from the models. The aim is to test if there is a statistical connection between current cometary abundances, and where and when such abundances were found in the pre-Solar nebula, thereby possibly tracing the formation histories of the comets. Based on this test, a possible "chemical evolution"-taxonomy of comets may be established if multiple comets match the same formation histories.

5.2   Methods

5.2.1   Model description

The modelled volatile ice abundances are taken from Eistrup et al. (2018). A physical disk model evolving in time was used featuring decreasing temperature and density structures from 0 to 30 AU, with the CO iceline residing inside 30 AU. Icelines (or snowlines) mark the radius in the disk midplane beyond which species exist solely in ice form and are thus depleted from the gas. This occurs at the radius where the accretion rate onto grain surfaces (or freezeout) exceeds the desorption rate from grain surfaces due to the negative temperature gradient in the midplane. The position of the midplane iceline for a particular species will depend on its volatility (i.e., its binding energy).

The disk structure used is not the pre-Solar nebula structure proposed by Hayashi (1981), and parameterised in Aikawa et al. (1997). However, the utilised

disk structure here is evolving in time, and chemical evolution model results are readily available from Eistrup et al. (2018). Besides, the locations in the disk important to comet formation are the volatile icelines, which are closer to the star for a colder disk, and further away from it for a warmer disk. Tracking comet formation based on iceline positions therefore means that the exact choice of physical disk structure is less important, and in addition, the 30 AU range of this disk covers all important icelines (including the CO iceline which starts just inside 30 AU).

Figure 5.1 shows a comparison of the midplane temperature and density structures from Hayashi (1981), and from Eistrup et al. (2018) (for the 0.1 MMSN disk by 1 Myr evolution), extending to 30 AU. The structures are different, in that the structure from Hayashi (1981) is warmer (roughly twice as high temperature at any radius) and more massive (more than ten times higher mass) compared to the disk from Eistrup et al. (2018) (hence the "0.1 Minimum Mass Solar Nebula"-designation for this disk). It is noted that the disk from Eistrup et al. (2018) has already lost mass by 1 Myr evolution, so in Fig. 5.1 the density difference between the disks is more than ten times. The disk mass of 0.1 MMSN from Eistrup et al. (2018) is the starting mass of the disk, not the mass by 1 Myr (as plotted in Fig. 5.1).

Results for the high ionisation rate are taken, which includes contributions from galactic cosmic rays, as well as decay products of short-lived radionuclei in the disk midplane (see e.g. Cleeves et al. 2013a; Padovani et al. 2018). A timescale up to 8 Myr is assumed for a long-lived gaseous protoplanetary disk. The high ionisation rate of typically $10^{-17}\mathrm{s}^{-1}$ means that chemical changes occur after a few 10^5 yrs. The disk structure cooling in time means that the volatile icelines move inwards in time.

Two different sets of initial abundances are assumed: inheritance and reset. Inheritance assumes all ices to have survived the trip from the parent molecular cloud to the disk midplane, thereby starting the chemical modelling with neutral molecules that are abundant in interstellar ices. The reset scenario assumes an energetic event to have dissociated all molecules into atoms (chemical reset) upon arrival in the midplane, thereby starting the chemical modelling with highly reactive atoms. This effect was proposed to happen in the hotter regions close to the protostar by e.g. Visser et al. (2009). The inner Solar System is assumed to have undergone some amount of chemical reset (with evidence from studies of chondrules and CAIs, see e.g. Trinquier et al. 2009), followed by a condensation sequence, depending on location in the disk. Comets, on the other hand, are often thought to be pristine, possibly because they formed, and mainly reside in the outer Solar System.

Colour maps of evolving abundances for different volatile ice species with respect to H_2O ice for both reset and inheritance scenarios are shown to the left in Figs. 5.6-5.10 in the Appendix. These plots allow an overview of when and where the different ice species are abundant. It can be seen that there are regions in the radius-time parameter space at which the modeled ice ratios well reproduce the observed ratios for most species. Based on these plots, the ice species considered in the statistical analysis are CO_2, CO, O_2, CH_4, C_2H_6, H_2S, OCS, SO_2, H_2CO and

CH$_3$OH. It is noted in each panel which molecule is considered, and whether the inheritance or the reset scenario has been assumed. To the right of the colour maps are shown the observed abundances of the given ice species in different comets. The ice species NH$_3$, HCN, HNCO, CH$_3$CN and C$_2$H$_2$ have all been detected and modelled, but they are excluded from the analysis. This exclusion is based on nitrogen ice chemistry in protoplanetary disks remaining poorly understood (see e.g. Schwarz & Bergin 2014; Walsh et al. 2015). Lastly, C$_2$H$_2$ is most likely to be a daughter species, and thus also not constraining the bulk cometary composition.

Daughter species in general have been excluded because the parent species are expected to be dominant in cometary ices, even if the daughter species are abundant in the comae. Since the daughter species in the coma originate from dissociated parent species in the gas after sublimation, the exclusion of daughter species means that the detected abundances of parent species in the coma are likely lower than the actual abundance on the cometary surface.

The detected abundances of each molecule in each comet are taken from Tables, 2, 3, 4 and 5 in Le Roy et al. (2015). If multiple values are given for the abundance of an ices species, then the median is used, and the difference between this median and the lowest given value is taken as the error. If only one abundance value was available, then a conservative error estimate of 50% of the observed value is assumed. This estimate is reasonable when compared with observed errors (see figures A1 to A5).

5.2.2 Statistical comparison between observations and models

With observed abundances of several molecules available for all comets, along with the evolving spatial midplane abundances of those molecules, it can now be quantified how likely it is for a comet to have formed at a given time and place, assuming that the comets acquired all their ices at one time and place, and that the ices remained unaltered thereafter.

For each comet, a log-space χ^2-surface in time t and radius r is computed. We do the analysis in log-space because of the large dynamical range (orders of magnitude) in the modelled abundances; hence, we consider a good agreement to lie within an order of magnitude of the observed ratio. For each set of radius r and time t, the χ^2 value for a given comet is given by

$$\chi^2(r,t) = \sum_{i=1}^{n} \frac{(\log(n_{i,\mathrm{obs}}(r,t)) - \log(n_{i,\mathrm{mod}}(r,t)))^2}{\sigma'_{i,\mathrm{obs}}(r,t)^2}, \tag{5.1}$$

where $n_{i,\mathrm{obs}}(r,t)$ and $n_{i,\mathrm{mod}}(r,t)$ are the observed and modelled abundance of species i with respect to H$_2$O ice at (r,t). $\sigma'_{i,\mathrm{obs}}(r,t)$ is defined as

$$\sigma'_{i,\mathrm{obs}}(r,t) = \max(|\log(n_{i,\mathrm{obs}}(r,t) + \sigma_{i,\mathrm{obs}}(r,t)) - \log(n_{i,\mathrm{obs}}(r,t))|,$$
$$|\log(n_{i,\mathrm{obs}}(r,t) - \sigma_{i,\mathrm{obs}}(r,t)) - \log(n_{i,\mathrm{obs}}(r,t))|) \tag{5.2}$$

where $\sigma_{i,\mathrm{obs}}(r,t)$ is the observed or estimated error on the abundance. We use this prescription as it is a more conservative estimate for the error when propagated using a log function. For the case where $\sigma_{i,\mathrm{obs}}(r,t) \ll n_{i,\mathrm{obs}}(r,t)$, one can estimate $\sigma'_{i,\mathrm{obs}}(r,t) \sim \sigma_{i,\mathrm{obs}}(r,t)/n_{i,\mathrm{obs}}(r,t)$; however, here, the errors are of the same order of magnitude as the measurement.

The χ^2-surface for each comet is then transformed into a maximum likelihood function $P(r,t)$ using

$$P(r,t) \propto e^{-\chi^2(r,t)/2} \tag{5.3}$$

and subsequently all sets of $P(r,t)$ for each comet are normalised by the maximum P-value for that comet. The resulting surfaces of maximum likelihood show contours of different colours in different regions of parameter space, with colours depending on how close a region is to the maximum likelihood value for the comet. Regions of parameter space close to the maximum likelihood value for a comet are in turn the regions showing best agreement between the chemical models and the observed cometary abundances.

These maximum likelihood (P-value) surfaces are shown for all comets in Fig. 5.2 which compares observations with models of the reset scenario, and in Fig. 5.3 for models of the inheritance scenario. The x-axes in each panel in each figure are radial distance from the star in AU, and the y-axes are chemical evolution time in Myr. For each contour level the value of the contour indicates where the fraction of the local P-value to the maximum P-value is above a certain level, for each comet. Regions of yellow contour indicate good agreement between models and observations, whereas darker colours indicate poorer agreements.

The comet names, and dynamical types from Cochran et al. (2012), are listed in all panels. In each panel is also given the number of molecular detections for each comet (from Le Roy et al. 2015), with the panels from left to right, and top to bottom featuring decreasing numbers of molecular detections per comet. This way, the first panel with ten molecular detections (Comet 67P-S) can be distinguished from the last panel with only two molecular detections (Comet 21P), in that more molecular detections in a comet should make the comparison between the models and the observations more robust.

5.3 Results

5.3.1 Full sample of species

5.3.1.1 Reset scenario

Fig. 5.2 features the maximum likelihood surfaces for the reset scenario with the full sample of species. For all comets, there are regions of the parameter space that show good agreement between models and observations. All comets are in good agreement with formation between 12-15 AU by ~ 8 Myr evolution, and most comets, excluding comets 67P-W, LINEAR and 17P, also show good agreement with formation between 27-30 AU by $\sim$0.5-1 Myr evolution. For comets Lemmon,

103P, 9P, 6P, 2P, and 21P, the two aforementioned regions of parameter space are connected with the contours at the chosen levels (down to 10^{-4} relative to the maximum likelihood value for each comet). For comets 103P and 2P there is a high degree of degeneracy in radius and time, as the maximum contours for these comets follow a trail spanning from the aforementioned 30 AU by $\sim$ by 1 Myr inwards to $\sim$ 12 AU by 8 Myr evolution. This trail is marked by the red shaded region overplotted for comet 2P, and this trail overlaps with the regions of highest likelihood for all comets, except for comet 17P.

The trail, in turn, roughly traces the CO iceline (at $T \sim 20$ K), as is seen in the left panel of fig. 4 in Eistrup et al. (2018). This figure, amongst others, shows the changing location of the CO iceline in the physically evolving disk midplane utilised in that work. This is interesting, because it points to all the comets here, except comet 17P, agreeing well with formation in the vicinity the CO iceline in the pre-Solar nebula.

Comet 17P, as an outlier, is seen to have several regions of parameter space in which it shows good agreement with formation. These regions are: 2-3 AU by 8 Myr, 5 AU by 0.5 Myr, 11 AU by both <0.5 Myr and by 8 Myr, and a large region at large radii at late evolutionary times. From this point of view, comet 17P is somewhat less constrained with respect to its formation time and location, than the other comets. Although comet 17P does show agreement over the regions of parameter space described above, it appears that this comet does not agree with formation along the CO iceline.

Additionally, all comets, except comets 73P, 6P and 2P, show high likelihood of formation at 5-10 AU by 7-8 Myr, which is roughly at the CH_4 iceline (see again fig. 4, left panel, in Eistrup et al. 2018).

5.3.1.2   Inheritance scenario

Turning to the inheritance scenario the maximum likelihood surfaces for all comets are presented in Fig. 5.3. All comets in this scenario share good agreement with formation at $\sim$ 12 AU by 8 Myr, similar to the case for the reset scenario in Fig. 5.2. All comets also show agreement with late formation (7-8 Myr) from small radii out to 10 AU, and some (103P, 6P, Lovejoy and 21P) also agree well with having formed inside 5 AU at various times during the evolution. The trail along the CO iceline that was seen for the reset scenario is not reproduced for all comets in the inheritance scenario. However, Hale-Bopp, LINEAR, Lemmon, 103P, 9P, 6P and 21P do somewhat agree with parts of the trail (103P and 6P are both in good agreement with the trail).

Most of the comets for the inheritance scenario also agree with formation at 25-30 AU by <1 Myr evolution. However, the best agreements between models and observations are for late evolutionary times. Comet 17P, as was the case for the reset scenario, does not showcase the same trends as the rest of the comets. Overall, the contours for 17P indicate that this comet is largely unconstrained in time and location.

Lastly, addressing both the reset scenario in Fig. 5.2 and the inheritance scenario in Fig. 5.3 it is generally seen that the more species that are observed in

a comet (the top panels of each figure), the smaller the regions in parameter space over which the models well reproduce the observed ratios, thus better constraining the potential formation location.

5.3.2   Correlation for C- and O-carrying species only

Given the interlinked chemical nature of carbon and oxygen, and the fact that the modelled nitrogen and sulphur chemistry is less well understood, it is interesting to have a look at maximum likelihood surfaces for the comets excluding sulphur species, and considering only ice species with carbon and oxygen. In the sample of molecules from Le Roy et al. (2015) these species are: C_2H_6, CO_2, CO, H_2CO, CH_3OH, CH_4 and O_2, thus seven in total.

For these seven ice species maximum likelihood surfaces are shown in Fig. 5.4 for the reset scenario and in Fig. 5.5 for the inheritance scenario. Since sulphur species have only been observed for comets 1P, Hale-Bopp, Hyakutake, LINEAR, 73P, 9P and 67P (both seasons), only these comets are relevant to analyse for differences compared to the analysis with the full sample of species.

Comparing these maximum likelihood surfaces to their counterparts in Fig. 5.2 for the reset scenario and Fig. 5.3 for the inheritance scenario reveals that excluding sulphur species does not significantly change the behaviour in the results. The only apparent difference is found comet Hale-Bopp, which in the reset scenario in Fig. 5.4 without sulphur agrees more broadly with formation at various evolutionary times and locations (though still along the CO iceline) than it did when including sulphur. However, this makes sense because excluding species from the analysis should cause less constraints on the most likely time and location of formation.

5.4   Discussion

Studies of comets and cometary compositions so far have been grouping them by either dynamical characteristics (length of orbit or inclination), or by their molecular contents (see Cochran et al. 2012). A'Hearn et al. (1995) and Cochran et al. (2012) defined standards for molecular abundances ("Typical"), such that cometary measurements could then indicate either enhanced or depleted abundances for a given molecule. While this approach does provide a grouping for comets that fit with the standard, it fails to include the possible chemical evolution of the comet-forming material in setting that standard.

This work attempts to trace the formation histories of 15 comets, by comparing cometary abundances with evolving ice abundances in a protoplanetary disk midplane through statistical tests. This way, rather than simply comparing similarities in the cometary contents, the potential formation times of the comets can also be addressed, since the chemical composition of the comet-forming disk midplane evolves over time. Four different comparison setups were investigated, with two different sets of observed abundances (either including or excluding sulphur-bearing species), and two different models for evolving abundances for the midplane (the
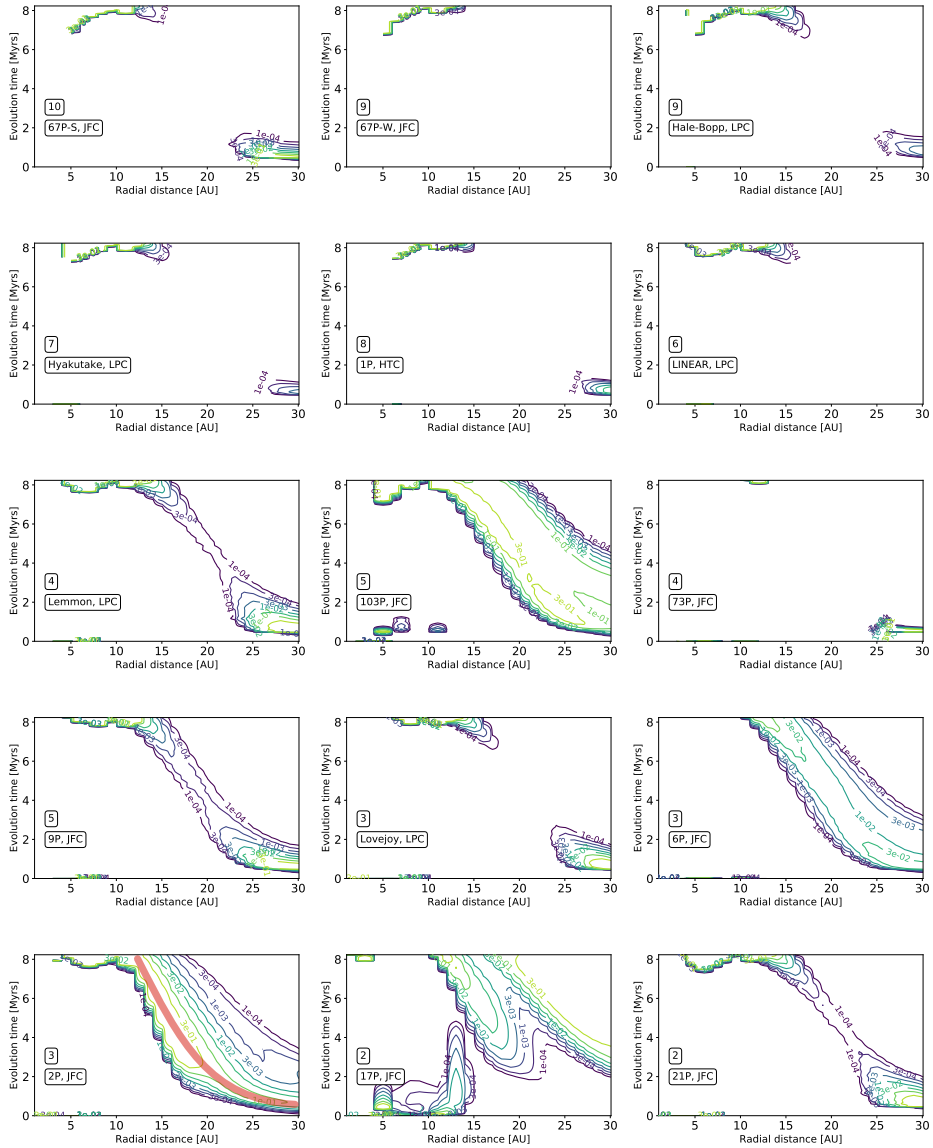
Figure 5.2: Maximum likelihood surfaces for the reset scenario, for the full sample of molecular species. Radius in AU in the physically evolving protoplanetary disk midplane is on the x-axis, and evolution time in Myrs is on the y-axis. The red shaded region for comet 2P indicates the trail through parameter space (largely tracing the vicinity of the CO iceline) on which most of the comets show good agreement with formation.
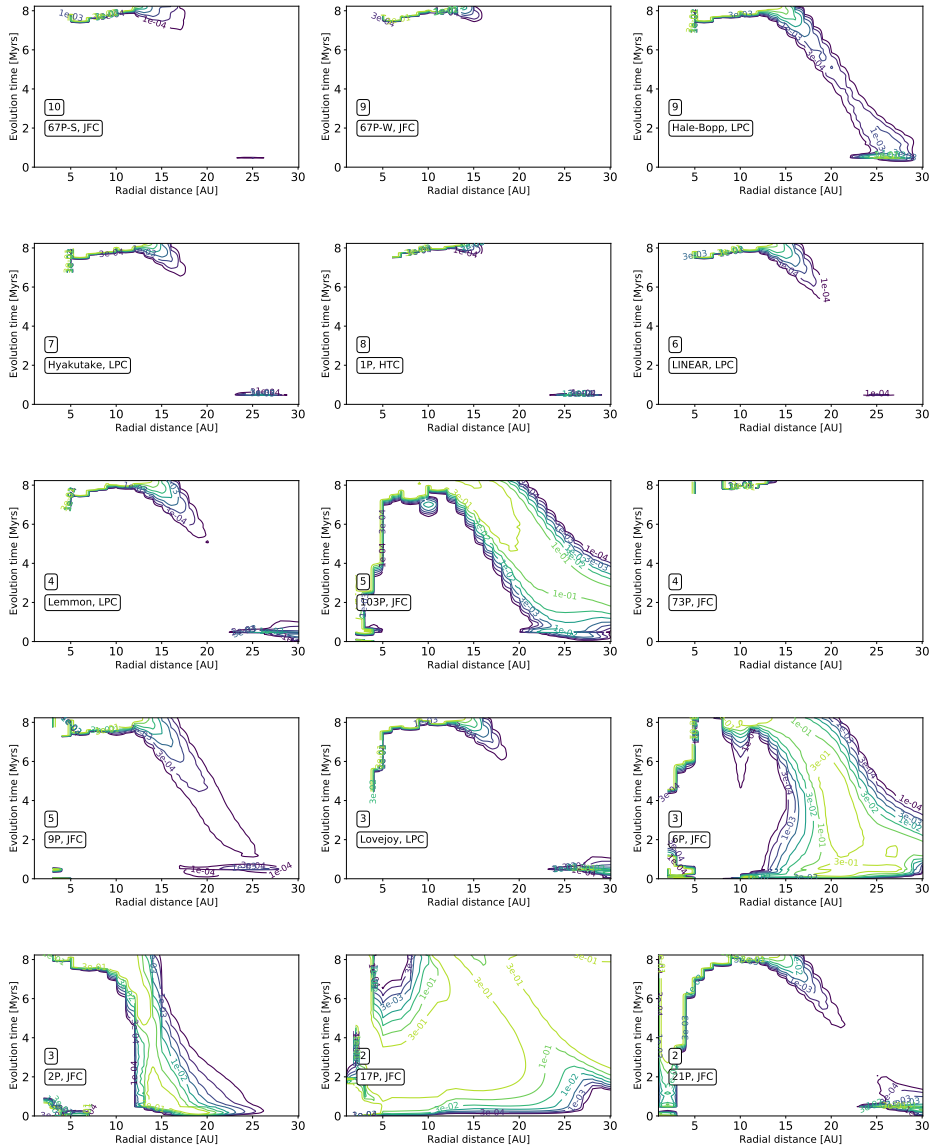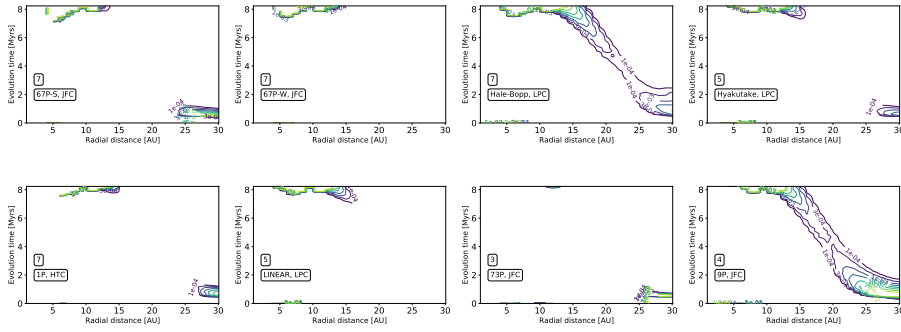
Figure 5.3: Maximum likelihood surfaces for the inheritance scenario, for the full sample of molecular species. Radius in AU in the physically evolving protoplanetary disk midplane is on the x-axis, and evolution time in Myrs is on the y-axis.
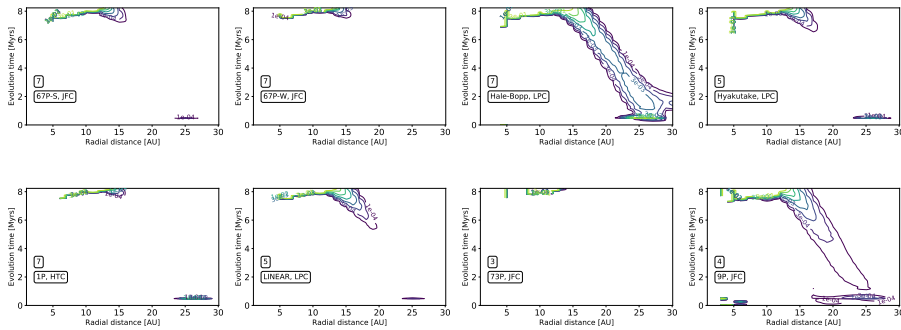
Figure 5.4: Maximum likelihood surfaces for the reset scenario, considering C and O bearing species only. Radius in AU in the physically evolving protoplanetary disk midplane is on the x-axis, and evolution time in Myrs is on the y-axis.

Figure 5.5: Maximum likelihood surfaces for the inheritance scenario, considering C and O bearing species only. Radius in AU in the physically evolving protoplanetary disk midplane is on the x-axis, and evolution time in Myrs is on the y-axis.

inheritance or the reset scenario).

For the reset scenario, good agreement is seen for formation along the CO iceline for 14 out of 15 comets. Comet 17P/Holmes remains largely unconstrained. Note that this comet underwent a so-called extraordinary outburst event (Santana 2007) prior to the observations compiled in Le Roy et al. (2015) (from Dello Russo et al. 2008). Dello Russo et al. (2008) found enhancements in HCN, C_2H_6 and C_2H_2 (by a factor of two to three) relative to other cometary observations; however, it is clear that cometary activity will have a great impact on the bulk composition derived from coma observations (see discussion later regarding comet 67P). The cause of the outburst event for comet 17P remains unknown.

The comets with more species observed in them are constrained to either formation at 27-30 AU by ~ 1 Myr evolution, or to formation at ~ 12 AU by 8 Myr evolution. Comets with fewer observed species agree well with formation along the CO iceline, as indicated by the red shaded region overplotted on the panel for comet 2P in Fig. 5.2. From the left panel in fig. 4 from Eistrup et al. (2018), 30 AU is by 0.5 Myr just outside the CO iceline (at 27 AU), which moves to 15 AU by 8 Myr. The CH_4 iceline is found at 10 AU by 8 Myr. For these 14 out of 15 comets this suggests that cometary formation can be constrained to lie roughly between the icelines of CH_4 and CO, with some degeneracy remaining in the formation time.

For the inheritance scenario, both with and without sulphur-bearing species, the results do not point as strongly to formation along the CO iceline, as is the case for the reset scenario. There is a similarity between the reset and inheritance scenario with good agreement for formation at 10-15 AU by 8 Myr, but this should be seen in the light of the results from Eistrup et al. (2018). It is shown there that the ice abundances for both scenarios tend towards icy disk midplane steady state at late evolutionary times (>5 Myr). That means that the ice abundances after 5 Myr evolution are largely similar across the two scenarios, resulting in similar maximum likelihood surfaces for both (see also the abundance evolution surfaces in Figs 5.6 -5.10).

Generally, the inheritance scenario does not point to a single formation history for all comets, but rather good agreement is seen for multiple formation regions in parameter space, and overall this scenario seems less constraining. This may indicate that our starting molecular abundances for the inheritance scenario do not resemble well those for the particular molecular cloud from which the Sun formed. Although this set of abundances are motivated by observations of ices in protostellar (or interstellar) environments (see Eistrup et al. 2016), it is possible that the Sun formed in a different (warmer) environment to that for nearby well-studied protostellar sources (see e.g. Adams 2010). It would be worth to explore the impact of a warmer interstellar environment on the initial inherited molecular abundances for a comet-forming disk.

Using the analysis here as a test of which chemical starting conditions and evolution best agree with the observations, the reset scenario is seen to generally agree best with the cometary observation. This scenario constrains all but one comet to most likely having formed in the vicinity of the CO iceline. As this iceline resides at a temperature at which grain-surface (ice) chemistry is particularly active, large

changes in the relative abundances of the volatile ice species are seen over time (see Eistrup et al. 2018). This active chemistry could in turn explain the diversity of observed cometary abundances.

That the reset scenario provides better constraints on location and time for comet formation, points to the comet-forming region in the pre-Solar nebula having been seeded with chemically processed material. This chemical processing can have several origins including an accretion shock *en route* into the forming disk, turbulent mixing within the disk once formed, or an accretion outburst caused by material in-falling from the disk onto the star. If any (all) of these processes have occurred, then this supports an early formation of comets (<1 Myr). However, if the pre-Solar nebula formed and evolved in a quiescent manner, a late formation of comets (~ 8 Myr) is also supported. In this latter case, it cannot be distinguished whether or not the cometary material has an interstellar origin.

Comparing the grouping of 14 comets here with the previous cometary classifications from Cochran et al. (2012) as "Typical", "Depleted" or "Mixed classification" (as of Table 2 in Le Roy et al. 2015) they fall under all these three classes. These 14 comets have thus never been grouped chemically together before. With these 14 comets now grouped together based on likely formation in the vicinity of the CO iceline, it is also possible to propose a formation sequence for this group, based on the peak of the maximum likelihood functions in Fig. 5.4.

Based on this, the following formation time classes from early to late for the 14 comets can be proposed: 67P-S, 73P, 21P, 9P, Lemmon and Lovejoy (all comets feature maximum likelihood peaks from 0.4-0.64 Myr at 28-30 AU), 2P and 103P (by 4.3-7.5 Myr at 14-16 AU), and Hyakutake, LINEAR, 67P-W, 6P, Hale-Bopp and 1P (by 8.23 Myr at 12-13 AU). It is noted that some of these comets have their maximum likelihood peaks located outside of the formation region around the CO iceline. For the sake of focusing on the possible formation time classification around this iceline, only likelihood peaks happening between 0.4 and 8.23 Myr were used for the analysis, thereby ignoring peaks outside of the CO iceline region of the parameter space. This formation time classification creates one group of six comets that possibly formed early, between 0.4-0.64 Myr, one that formed possibly at an intermediate time by 4.3-7.5 Myr, and another group of seven comets that possibly formed later after 7.5 Myr. This hints that comet formation may occur in tandem with disk evolution over ~ 8 Myr timescales.

This formation classes should be considered in light of which comets have more detections. As is evident in Fig. 5.4, the maximum likelihood peaks are very localised (either ~ 14 AU by 8 Myr or at ~ 30 AU by 1 Myr) for the comets that have more detections. The comets with fewer detections are less constrained and thus have larger regions of parameter space with good agreement with the models. The comets with more detections are thus constrained to having formation times similar to each other.

An interesting additional consideration regards which specific species have been detected in which comets, and how that may relate to which regions of parameter space the comets are in best agreement with, and how that may relate to the regions of best agreement in parameter space. Comets 73P, 2P, 9P, 6P and 17P have no CO detections in them, yet in the analysis here these are all constrained to

have formed in the vicinity of the CO iceline. Detection of CO in a comet is thus not a pre-requisite for constraining the comet formation (roughly) to this region. Note that a comet that has formed inside of the CO ice line will naturally be CO poor.

Lastly, it is seen from all plots of comet 67P-S and 67P-W that the summer and winter sides of the comet feature different compositions. Which side, or which relative proportions of the sides are representative of the bulk composition of the comet is still unclear, as was noted in Le Roy et al. (2015). Given that the two seasons of comet 67P fall into different formation classifications (67P-S agrees with early formation, whereas 67P-W agrees with late formation), classifying the formation time of the comet as a whole should be done with caution, although the summer side observations of the comet are likely more comparable to the observations of the other comets. One reason for the differences between the two seasons around 67P, could be that the temperature on its winter side is too low for H_2O ice to sublimate. This, in turn, can lead to increased abundances of the rest of the molecular species, because the all have a lower sublimation temperature than H_2O ice. This is important evidence that cometary activity is an crucial factor to take into consideration when extrapolating abundances measured in the coma to the bulk composition. In future work, it would be worth to explore how the ice ratios vary relative to a different species that is less susceptible to summer and winter effects.

5.5   Conclusion

In this work a statistical χ^2 method has been used to perform a quantitative comparison between observed cometary abundances and modelled chemical evolution in a protoplanetary disk midplane, by computing maximum likelihood surfaces, as a function of disk midplace location (radius) and time. The best agreements between observed and modelled abundances were found when considering the chemical evolution models to be chemically reset at the start, thus assuming that the volatile content of the pre-Solar nebula was (perhaps partially) atomised before dust grains starting building larger bodies. This is consistent with the traditional idea about the chemical start of the inner pre-Solar nebula (Grossman 1972).

Out of 15 comets, 14 were found to have high likelihoods of formation along a trail in time and radial parameter space consistent with the position of the CO iceline. Since CO is the molecule (next to N_2 and H_2) with the lowest binding energy (E_b=855 K) this means that most molecules are in the ice at the point where the comets are most likely to have formed. We do not consider here formation radii outside of the CO iceline, as the abundances in this region are found to be very different from those around the iceline (see Eistrup et al. 2018). There, it is found that the grain-surface chemistry is mainly driven by hydrogenation reactions leading to high abundances of e.g., H_2O, CH_4, C_2H_6, and CH_3OH ices.

Based on the maxima of the likelihood functions for each comet along the CO iceline, it was then determined when during chemical evolution each comet was most likely to have formed. Thereby a formation time classification for 14 comets

was proposed, with some degeneracy remaining between the early (<1 Myr) and late (>7.5 Myr) formation. With more samples of comets with sufficient molecular detections in the future, it will be possible to further test this chemical evolution classification scheme for formation histories of comets. It will be interesting to see if other comets support the idea of a chemical reset start, and if they too show best agreement with formation in the vicinity of the CO iceline.

5.A   Evolving modelled abundances and cometary abundances

This appendix features abundance ratio maps (Figs. 5.6-5.10) in radius and time for the molecular species considered in this work, as well as HCN, NH_3, HNCO, CH_3CN and C_2H_2. These abundances are taken from Eistrup et al. (2018). Each row is for one molecular ice species. The left columns of the figures are evolving abundances for the reset scenario ("Atomic"), and the middle columns for inheritance scenario ("Molecular") from the 0.1 MMSN evolving disk from Eistrup et al. (2018). The right column features the observed abundances (with given errors, or, if no error was given, assuming a conservative 50% error relative to the observed species abundance with respect to H_2O ice) of a given ice species, in those of the 15 comets, where the molecule has been observed.

The colourbar next to the right column indicates that high abundance with respect to H_2O ice gives a light colour, and low abundance gives a darker colour. The cometary abundances can also be read off vertically on the y-axis. The colour abundances of the comets are intended to enable easy visual comparison between the modelled (left and middle columns) and observed (right column) abundances.
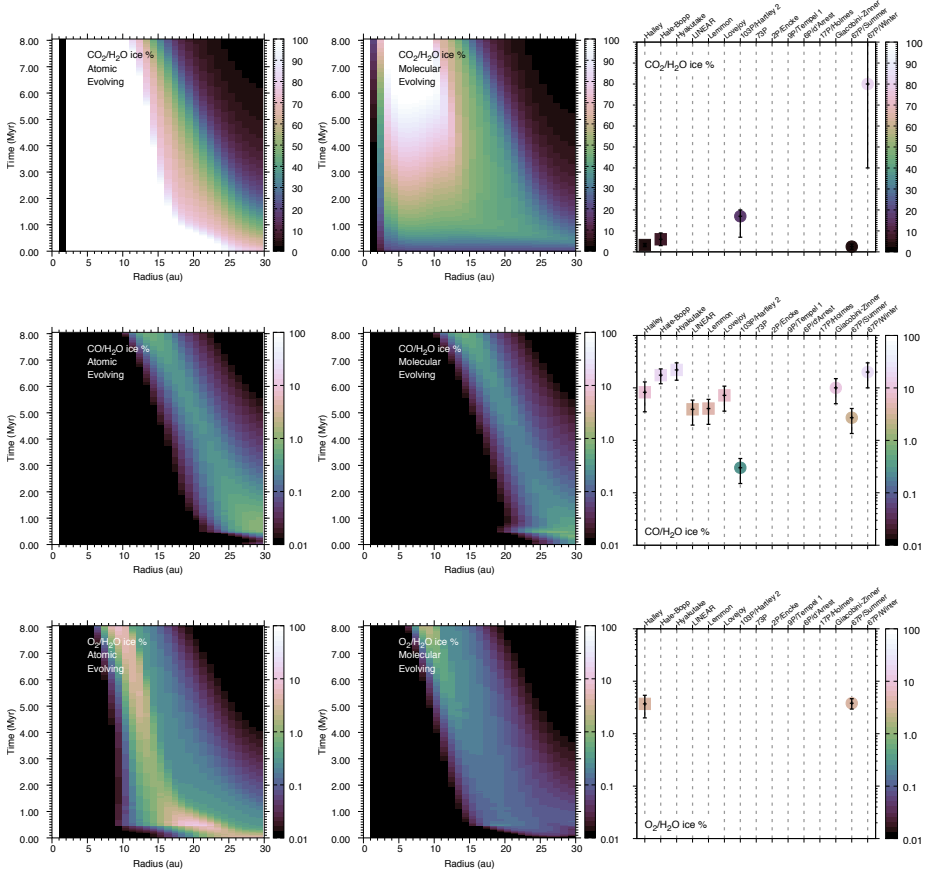
Figure 5.6: Abundance of CO_2, CO, and O_2 ice relative to water ice as a function of radius and time for the protoplanetary disk model with evolving physical conditions and using fully atomic initial abundances (left) and fully molecular initial abundances (middle). Note that the data for CO_2 are shown on a linear scale as opposed to logarithmic because of the low dynamic range in the chemical model results. The right-hand column shows the corresponding values measured for each species in cometary comae. The vertical dashed lines are included solely to guide the eye. Oort cloud comets and Jupiter family comets are represented by the squares and circles, respectively. For comets without a stated observed error (or range), we have assumed a conservative error of 50% of the observed ratio with respect to H_2O ice.
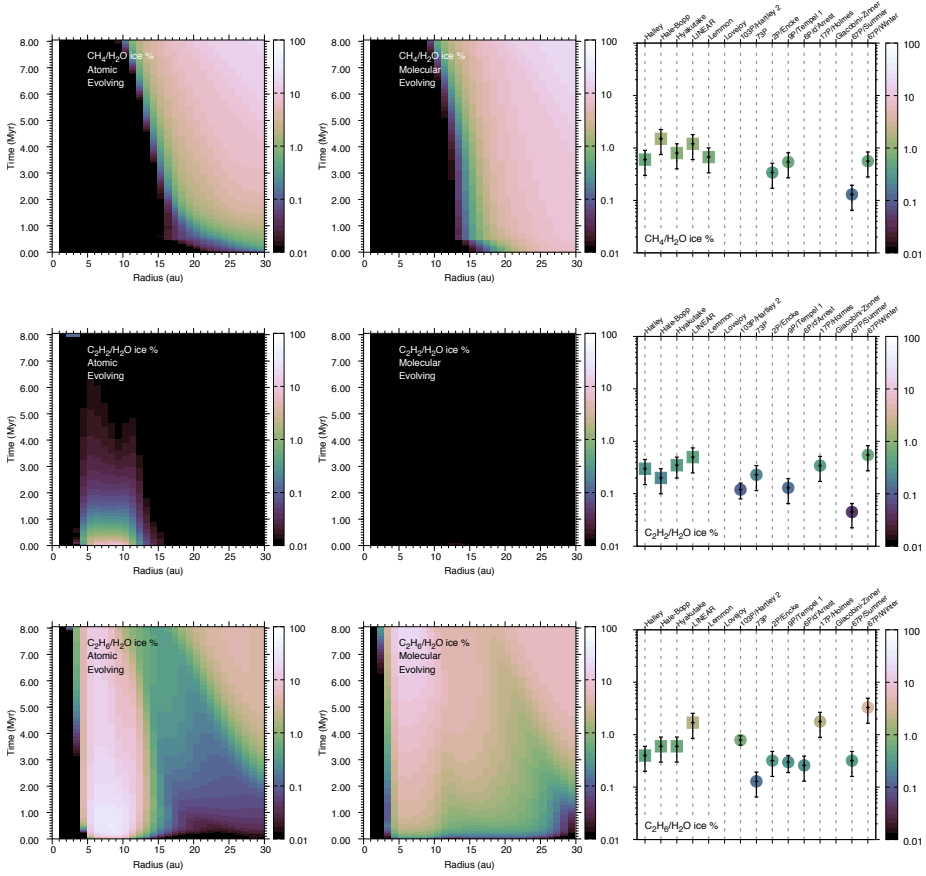
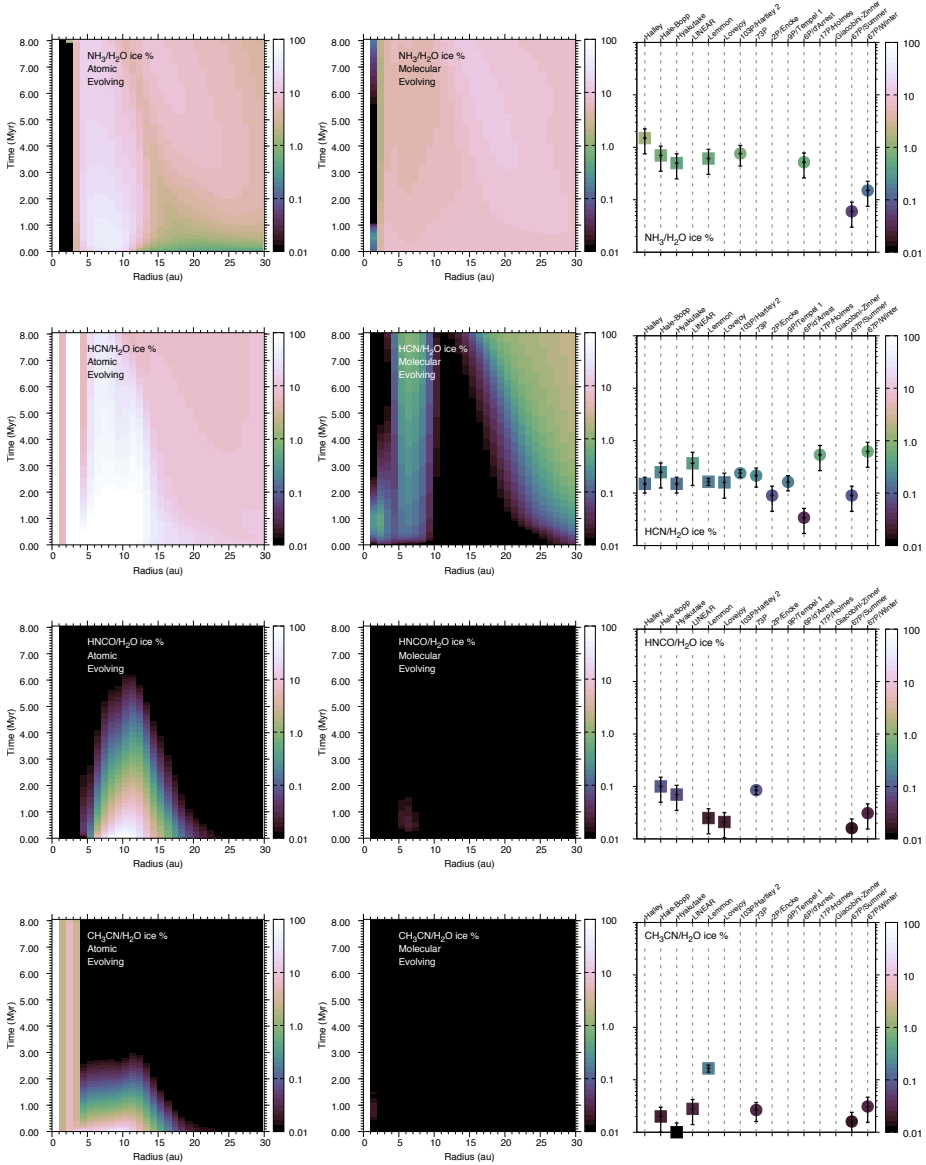**Figure 5.7:** Same as Figure 5.6 for CH$_4$, C$_2$H$_2$, and C$_2$H$_6$ ice.

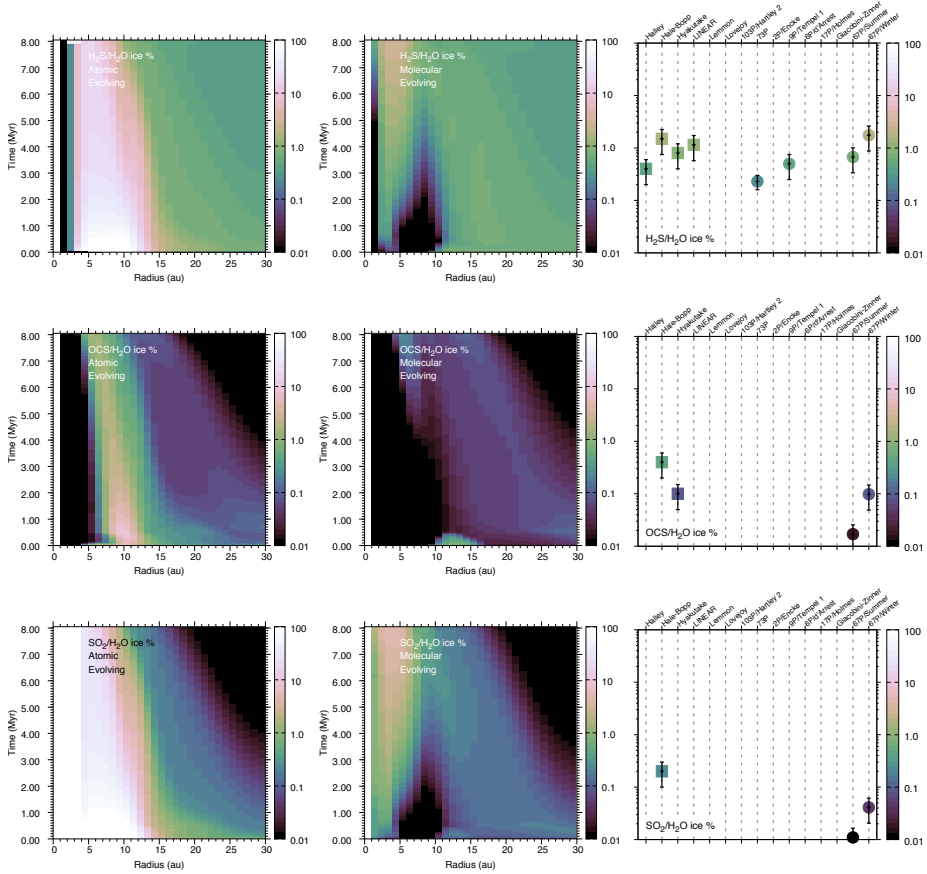**Figure 5.8:** Same as Figure 5.6 for NH$_3$, HCN, HNCO and CH$_3$CN ice.

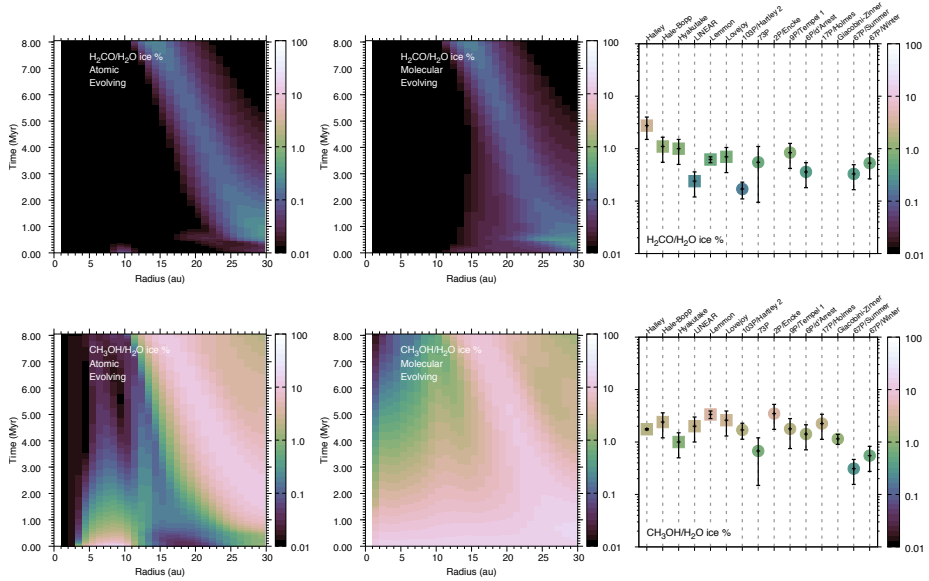**Figure 5.9:** Same as Figure 5.6 for H_2S, OCS, and SO_2 ice.

Figure 5.10: Same as Figure 5.6 for H$_2$CO and CH$_3$OH ice.